A Design Methodology for Hysteretic Dampers

by

Bora M. Tokyay

B.S., Lafayette College, PA (2001)
A.B., Lafayette College, PA (2001)

Submitted to the Department of Civil and Environmental Engineering
in partial fulfillment of the requirements for the degree of

Master of Engineering in Civil and Environmental Engineering

at the

MASSACHUSETTS INSTITUTE OF TECHNOLOGY

June 2002

Author .....
Department of Civil and Environmental Engineering
May 15, 2002

Certified by .....
Jerome J. Connor
Professor of Civil and Environmental Engineering
Thesis Supervisor

Accepted by .....
Oral Büyüköztürk
Chairman, Department Committee on Graduate Students

A Design Methodology for Hysteretic Dampers

by

Bora M. Tokyay

Submitted to the Department of Civil and Environmental Engineering
on May 15, 2002, in partial fulfillment of the
requirements for the degree of
Master of Engineering in Civil and Environmental Engineering

Abstract

In this thesis, a design methodology for hysteretic dampers, which are energy dissipation devices for buildings, is proposed. The increasing repair and insurance costs in the construction industry suggest a trend towards following a damage-controlled design philosophy in which the motion of the structure is the design parameter, as opposed to strength. Damage-controlled structures consist of energy dissipation systems, such as hysteretic dampers, in addition to the primary structural elements. The proposed design methodology is developed and explained using a typical building and then evaluated by running computer simulations.

Thesis Supervisor: Jerome J. Connor
Title: Professor of Civil and Environmental Engineering

Acknowledgments

Thank you all.

In order of appearance:

Mom and Dad – for getting it ALL started

My big brother – for being proud of me

Teachers at Robert College – for setting up the strong foundation

RC'97 – for helping me be who I am

YAH'97 – for not letting me forget who I am

Profs at Lafayette – for helping me get here

Prof. Saliklis – for making me a structural engineer

Friends at Lafayette – for making me have a great four years

MIT – for not being as bad as I thought you would be

Special Thanks to...

Prof. Connor – for broadening my horizons and making me see the Big Picture

Franny – for being and saying "canım benim"

Kevin – for too many things

Carmen – for our not "supposed to be had" conversations

Fiona – for your sweet tone of speech

Marc – for understanding

Charisis – for being aaa, you know.... aaaa. He he he..

Tzu-Yang – for being the Master

Paul – for your valuable procrastination skills

Lisa – for winning our love

Onur – for the fresh food, the clean fridge, the clean room

It sure was a crazy nine-months here at MIT. Never thought I would be sad leaving this place, but somehow you guys just managed to make me. Until we meet again,

enjoy,

bora

Contents

List of Figures

List of Tables

Chapter 1

Introduction

The advances in the practice of earthquake engineering, coupled with the increased use of sophisticated computer analysis tools, have led engineers around the world to consider the use of energy dissipation devices in both large- and small-scale structures. These seismic energy dissipation devices are passive control devices that provide reliable sources of seismic energy absorption.

There are a number of energy dissipation or damping mechanisms currently available for structural engineers. Some of the most common ones are viscous dampers, frictional dampers, tuned-mass dampers, viscoeleastic dampers and hysteretic dampers. The design methodology presented in this thesis is for hysteretic dampers. As such, hysteretic dampers will be investigated in greater detail in the following sections.

The use of damping mechanisms, hysteretic dampers in specific, to control the response of a structure is not limited to new buildings. In fact, the use of damping mechanisms in retrofit applications is gaining more popularity and acceptance everyday. A good example to that is the Seismic Retrofit of the Wallace F. Bennett Federal Building in Salt Lake City, UT. Although the reinforced concrete structure was designed and constructed according to the codes that prevailed during its time of construction in the 1960s, the advances in seismic resistant design show that the building would not be capable of resisting the large magnitude earthquakes the nearby Wasatch Fault could generate [4]. The use of hysteretic dampers was found appropriate for that particular project considering parameters and constraints such as cost,

aesthetics and continuous functionality of the building during construction.

The Bennett Building is not the only structure that does not comply with the current building codes. In fact, the number of such structures is so large that Federal Emergency Management Agency (FEMA) funded a study to address this issue and arrive at feasible rehabilitation methods for such buildings. To achieve this goal, following a detailed investigation of numerous structures, FEMA identified several model buildings for analysis purposes according to parameters such as height and location.

In what follows, the concept of Damage Controlled Structures and the associated design philosophy will be introduced first. Following that, the thesis describes the mechanics of how hysteretic dampers work and then introduces three design methodologies for retrofitting buildings with dampers. These methodologies are applied to a three-story building located in Los Angeles to provide a basis for comparison. Although a rehabilitation strategy is the main interest of this thesis, the proposed design methodology is not restricted to retrofit applications and can be adapted for new buildings.

The optimal stiffness and damping combination from the Analyses section will be taken as inputs for the nonlinear analyses. The methods and simplifications used to model the structure and the associated difficulties that arose in the process are included to provide insight for further work.

The thesis concludes by addressing an important aspect of the rehabilitation process; the cost. The cost analysis is reduced to material cost calculations and finding the relative importance of each element in a rehabilitation project where hysteretic dampers are utilized.

Chapter 2

The Design Philosophy

2.1 Introducing Damage Controlled Structures

An optimal design for a building is the one that satisfies the predefined safety and serviceability requirements for the minimum amount of cost. Historically strength based design has been followed in practice. The current building codes, such as the Uniform Building Code, are based on the strength based design philosophy, in which the structure is designed with respect to strength constraints. The stiffness properties of the structure are established according to strength requirements, and then the building is checked for serviceability criteria. Usually an iterative process is necessary to obtain an acceptable design that satisfies both sets of requirements. This kind of design results in a structure in which the stiffness and energy absorption mechanisms are combined in one, as a result of which the building deforms inelastically.

Strength based design has been appropriate in the past where strength was the dominant design requirement. However, recent developments, especially the increase in repair and insurance costs suggest a new design philosophy should be used, one that minimizes the damage in the structure. Proposed by J. J. Connor[1] and A. Wada[2], a damaged controlled structure is "a combination of several structural systems and energy transformation devices that are integrated in such a way as to restrict damage

[1]Massachusetts Institute of Technology, Cambridge, MA
[2]Tokyo Institute of Technology, Tokyo, Japan

to a specific set of structural elements that can be readily repaired" [8]. The justification of using damage-controlled structure is depicted in Figure 2-1, taken from [8], which relates the repair cost to earthquake intensity for a conventional structure and a damage-controlled structure. The figure indicates that damage-controlled structures are most effective for moderate earthquakes.

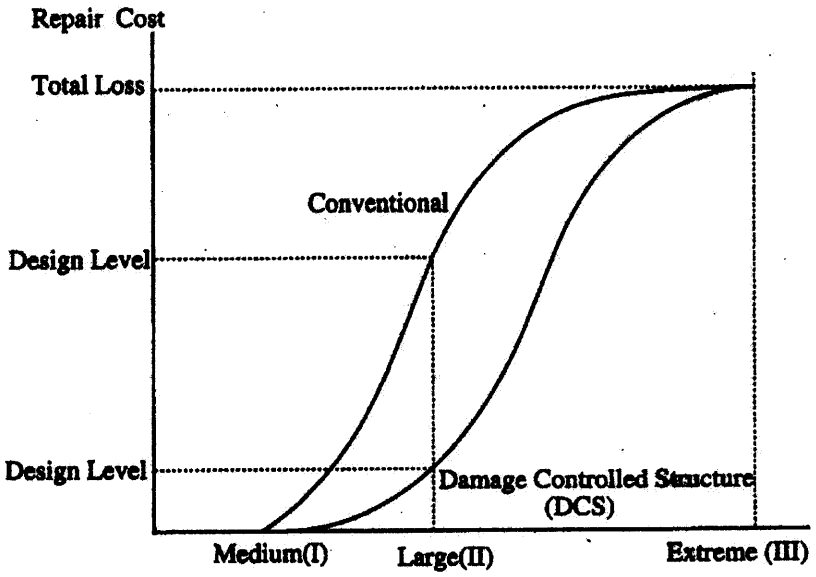

Figure 2-1: Repair Costs vs Earthquake Intensity for Conventional and Damage-Controlled Structures.

Since the main reason for damage is motion, creating a damage-controlled structure involves controlling the motion of the structure. Connor and Wada argue in their earlier works [9], [7] that the spatial distribution of the structure's motion (i.e. the modal shape) is determined by stiffness, while the amplitude of the motion is a function of both stiffness and energy absorption (or damping). Therefore in the design methods that are presented in this thesis as alternatives to strength based design, first the stiffness distribution that yields the desired displacement profile is obtained, and then the damping is added to adjust the magnitude of the response. It is worth remembering that the damping or energy absorption mechanism is separated from the primary system that provides both lateral and vertical support. Figure 2-2 depicts

the concept graphically. The structure (a) consists of (b) the primary structure and (c) the damping system.

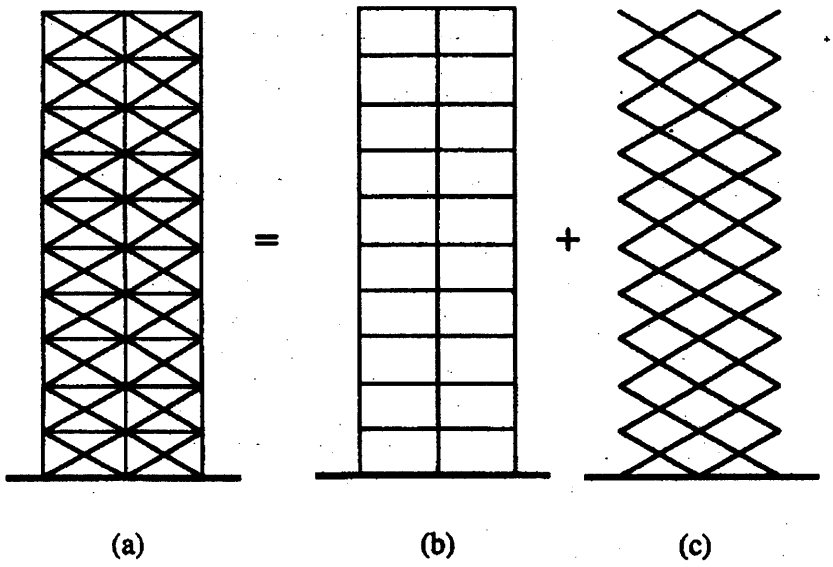

Figure 2-2: Concept of Damage Controlled Structures: (a)Actual Structure; (b)Primary Structure; (c)Damping System. Taken from [8].

2.2 Establishing the Design Standard

In October of 1997, Federal Emergency Management Agency (FEMA) released FEMA-273: NEHRP Guidelines for the Seismic Rehabilitation of Buildings. This document, which will be referred to as the *Guidelines*, is the latest and most appropriate standard for any rehabilitation project. The *Guidelines* detail the requirements and steps of a systematic retrofit for a broad range of building types, performance levels, and seismic hazards.

One of the first steps in a rehabilitation process is to decide on a set of Rehabilitation Objectives for the building. Rehabilitation Objectives are "statements of the desired building performance when the building is subjected to earthquake demands of specified severity" [1]. Therefore in order to establish a set of Rehabilitation Objectives, the structural engineer needs to know about Performance Levels and Seismic

Hazard. Performance Levels Building performance can be described qualitatively in terms of several factors:

- The safety afforded building occupants during and after the event
- The cost and feasibility of restoring the building to pre-earthquake condition
- The length of time the building is removed from service to effect repairs
- Economic and architectural impacts on the larger community

In light of these factors, building performance levels and ranges are separated into two groups: Structural and Nonstructural. Since the main interest of this thesis lies in the *structural* problems caused by seismic excitations, the descriptions Performance Levels and Ranges are limited to those of Structural ones. In terms of notation, Structural Performance Levels are denoted by both names and numbers (following S-), while Nonstructural Performance Levels are identified by a name and an alphabetical designator (following N-).

2.2.1 Structural Performance Levels and Ranges

Three discrete Structural Performance Levels and two intermediate Structural Performance Ranges are defined. The Structural Performance Levels are the Intermediate Occupancy Level (S-1), the Life Safety Level (S-3), and the Collapse Prevention Level (S-5), while the Ranges are the Damage Control Range (S-2) and the Limited Safety Range (S-4). Acceptance criteria are well defined for the levels, while design parameters for the ranges need to be interpolated from the values obtained for the preceding and the subsequent performance levels. The relevant Performance Levels and Ranges are explained below based on the definitions provided in the *Guidelines*:

Immediate Occupancy Performance Level (S-1)

The post-earthquake damage state in which only very limited structural damage has occurred. The basic vertical– and lateral– force resisting systems retain nearly all of their pre–earthquake strength and stiffness.

Damage Control Performance Range (S-2)

Continuous range of damage states that entail less damage than that defined for the Life Safety Level, but more than that defined for the Immediate Occupancy Level.

Life Safety Performance Level (S-3)

The post-earthquake damage state in which significant damage to the structure has occurred, but some margin against either partial or total structural collapse remains. There might be injuries during the earthquake, however life-threatening injuries are very unlikely.

Limited State Performance Range (S-4)

Continuous range of damage states between the Life Safety and Collapse Prevention Levels.

Collapse Prevention Performance Level (S-5)

The building is on the verge of experiencing partial or total collapse. Substantial damage is done to the structural systems, including degradations in strength and stiffness in vertical and lateral force resisting members. However, all significant components of the gravity-load-resisting system must continue to carry their gravity load demands. The structure may not be technically practical to repair and is not safe for reoccupancy, as aftershock activity could induce collapse.

For more detailed explanation of the Structural Performance Levels and Ranges as well as information on Nonstructural Performance Levels, the reader is advised to visit Chapter 2 of the *Guidelines*, [1].

2.2.2 Seismic Hazard

Seismic Hazard presents methods for determining earthquake shaking demands. Earthquake demands are a function of the location of the building with respect to causative faults, the regional and site-specific geologic characteristics and the hazard level(s)

selected in the Rehabilitation Objective. In this study hazard levels defined on a probabilistic basis are used, which state the probability that more severe demands will be experienced (probability of exceedance) in a 50-year period. Hazard levels used in this study are given below:

Earthquake having probability of exceedance	Mean Return Period (years)
50%/50 year	72 (rounded to 75)
10%/50 year	474 (rounded to 500)
2%/50 year	2475 (rounded to 2500)

In the *Guidelines*, and also in this thesis, frequent reference is made to two levels of earthquake hazard that are useful for the formation of the Rehabilitation Objective. These are termed Basic Safety Earthquake 1 (BSE-1) and Basic Safety Earthquake 2 (BSE-2). They are taken as 10%/50 and 2%/50, respectively. Appendix A includes tables of basic characteristics of Los Angeles Ground Motion Records. Taken from FEMA-355C, this table provides a set of earthquake excitations for the hazard levels mentioned above. In the examples given in this thesis the Imperial Valley, 1940 earthquake is taken as the representative earthquake and is scaled up to a peak ground acceleration (PGA) of 261.0 in/sec^2 (6.63 m/sec^2) for BSE-1. The same earthquake is scaled up to a PGA of 391.5 in/sec^2 (9.95 m/sec^2) to be used as BSE-2. Figure 2-3 shows the time history record of the acceleration for the Imperial Valley, 1940 earthquake as well as its scaled up versions corresponding to BSE-1 and BSE-2. The time history data for this earthquake were obtained from the University of California, Berkeley Website.

Three levels of objectives are specified in the *Guidelines*, Basic Safety Objective (BSO), Enhanced Rehabilitation Objectives and Limited Rehabilitation Objectives. In order to achieve BSO the building rehabilitation must be designed to attain the Life Safety Performance Level for BSE-1 and the Collapse Prevention Level for BSE-2 earthquake demands. A structure that is retrofitted to provide a performance superior to BSO is said to have an Enhanced Rehabilitation Objective. Conversely if the goal of the retrofit is to provide a performance inferior to BSO, the Rehabilitation Objective is called Limited. It should be noted that structures designed and constructed in

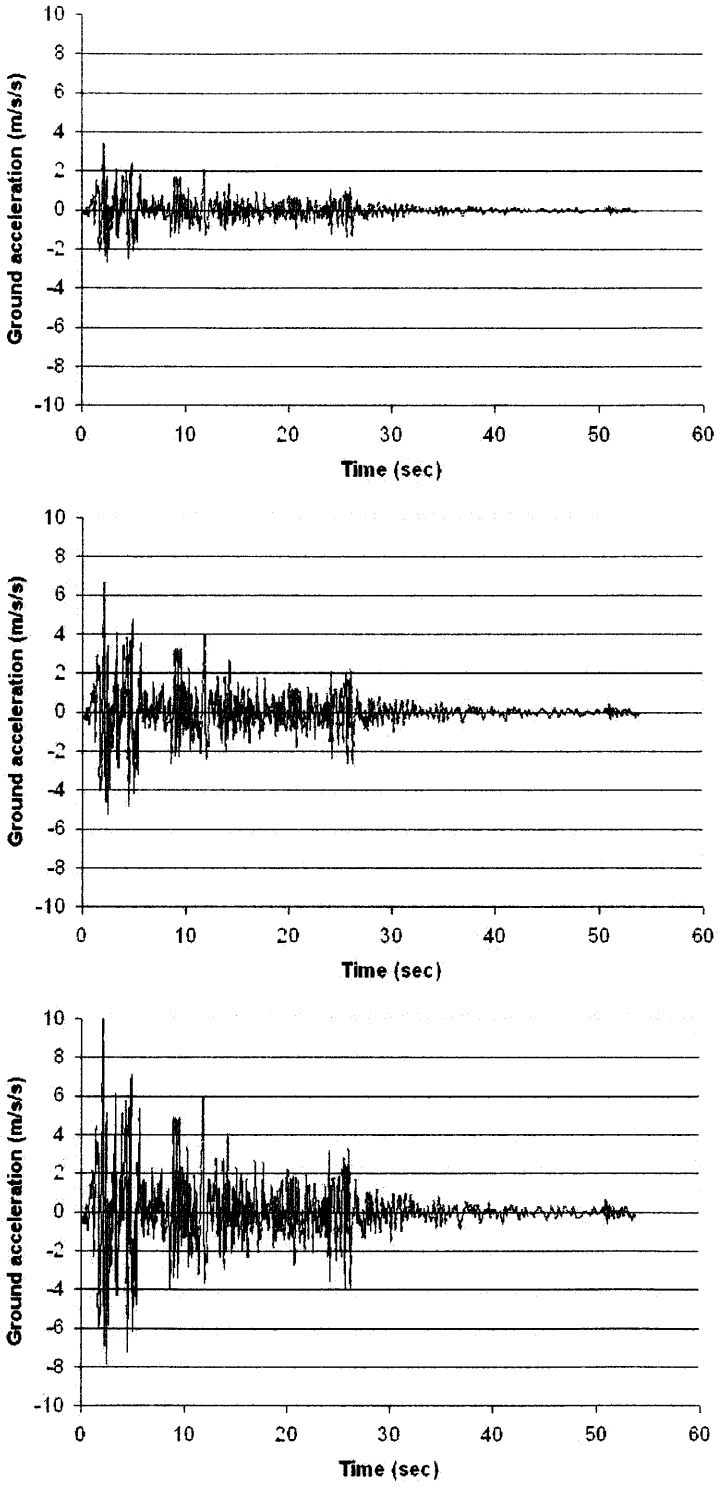

Figure 2-3: Time history plots of the ground acceleration for Imperial Valley, 1940 earthquake and its BSE-1 and BSE-2 versions.

accordance with the latest building codes, namely BOCA 1993, SBCC 1994, ICBO 1994, may be deemed to meet the BSO.

Since the *Guidelines* provide a formal procedure to be followed only for BSO, it is suggested that according to FEMA attaining BSO should be the goal of a typical rehabilitation project. However, in light of Connor's and Wada's work on the significance and benefits of keeping the damage on the structure within economically repairable limits, and the definitions of the performance levels the BSO corresponds to, selecting BSO as the primary objective is deemed inadequate.

Therefore the Rehabilitation Objective set for this thesis consists of attaining Immediate Occupancy Performance Level for BSE-1 and Collapse Prevention Performance Level for BSE-2 excitation. This objective would be considered as an Enhanced Rehabilitation Objective, and is likely to cause higher initial costs. However it is argued here that the initial higher costs will be offset by the savings in repair costs throughout the life of the structure.

The *Guidelines* have converted the qualitative descriptions of the Performance Levels into quantitative design criteria in terms of the allowable drift. According to these parameters, a structure consisting of Braced Steel Frames (which is the main structural system in the rehabilitated building in this thesis) can have 0.5% transient and negligible permanent drift for BSE-1 to satisfy the Immediate Occupancy Level and 2% transient or permanent drift for BSE-2 to satisfy the Collapse Prevention Level.

Chapter 3

Hysteretic Dampers

3.1 Applications of Hysteretic Dampers

To date, the use of hysteretic dampers has not been as popular in the United States as it has been in Japan, where this mechanism is used in more than 160 building [4]. However, there are reasons to believe its applications will gain popularity in the United States, especially in the seismic West Coast. Nippon Steel Corporation, the Japanese producers of the propriety low-yield strength steel used in the hysteretic dampers in Japan, are gradually entering the market in the West Coast. For instance, The Bennett Building, mentioned earlier in Section 1 is the first federally owned building to employ the buckling-restrained braces manufactured by Nippon Steel.

Table 3.1 below, modified from [10] lists some of the buildings in Japan where hysteretic damping systems are used. Two of the more interesting examples are briefly introduced below

Central Government Building

This 100 m high building serves as the headquarters for the Government Police Board and therefore has great importance. It is designed to behave elastically even under large intensity earthquakes. The hysteretic dampers used in this building are steel walls made of extra-low yield point steel (yield strength 100MPa). The Hysteretic Damping system is accompanied by an additional viscous damping system which

Table 3.1: Tall steel buildings in Japan designed using hysteretic dampers.

Year	Project Name	Location	Usage	Height (m)
1995-6	International Congress	Osaka	Congress	104
1995-8	Central Government	Tokyo	Office	100
1996-3	Passage Garden	Tokyo	Office	61
1996-6	Art Hotel	Sapporo	Hotel	96
1996-4	Shiba 3 Chome	Tokyo	Office	152
1998-5	Kouraku Mori	Tokyo	Office, Shop	82
1998-7	Harumi 1 Chome	Tokyo	Office, Shop	88
1998-4	East Osaka City	East Osaka	Office	120

consists of two movable steel plates and three fixed steel plates.

Passage Garden in Shibuya, Tokyo

This 61.4m building has 14 stories and no vertical columns. The entire structural system consists of two distinct systems; elastic column system and unbonded brace system (which provides hysteretic damping). The damage is clearly confined to the unbonded braces, which are installed in easy to replace locations.

3.2 How Do Hysteretic Dampers Work?

In pure frame elements (i.e. no braces, no dampers), the energy is dissipated through the yielding that occurs at the flange welded part of the beam ends for steel structures [10]. In essence the beam ends are "sacrificed" for the structural integrity of the whole building. However, the yielding that occurs at the end of the beams is not enough to dissipate all the energy that enters the system and therefore large deformations are inevitable in case of seismic excitations.

Underlying the use hysteretic damping mechanisms is the same philosophy of sacrificing a member or members to avoid excessive damage in the building. Unlike in pure frames however, the yielding occurs in the core elements of the unbonded-brace members, which are usually installed diagonally in the chevron or V configuration. The design of such an element involves ensuring adequate yielding to absorb the

required energy.

To ensure that yielding occurs at the specified locations (i.e. at the hysteretic elements) and not anywhere else in the building, the core element of the damper is designed to have a relatively low yield strength in comparison to the primary structural elements. Currently all applications of hysteretic dampers use an ultra low yield steel produced by Nippon Steel, Japan as the core material. Although the use of low yield strength steel may be desirable with respect to yield considerations, the low buckling strength of the member is an unwanted consequence of such a selection. The fact that these members have low yield strength naturally leads to a buckling problem, since these members experience both tensile and compressive forces. That is why unbonded-braces are introduced.

Figure 3-1 shows a hysteretic damper installed by Mori Building Company of Japan in a 44-story building. The low yield strength steel core is encased over its length in a steel tube which is filled with concrete. The steel tube sleeve or jacket restrains the inner core from buckling by providing extra bending rigidity. However, a slip interface, or an "unbonding" layer between the steel core and the surrounding concrete is necessary so that all the axial force is taken by the core element. Hence the material and the geometry of the slip layer must be such that relative movement is allowed between the steel core and the concrete considering shearing and Poisson's effects, but at the same time buckling is prevented as the core member yields in compression.

The name hysteretic dampers comes from the behavior these yielding elements exhibit under cyclic loading. Figure 3-2 shows the Load-Deflection plot obtained from the testing of a material that is used as a yielding core element. In this particular example the curves are for $\pm 0.4\%$ and $\pm 0.55\%$ strain cycles. The loops that form are called Hysteresis loops, hence the name, hysteretic damper.

Extensive testing has been done both in University of California, Berkeley and Japan on unbonded-braces to produce repeatable symmetric behavior in tension and compression, up to ductility ratios of 15-20 [4], where ductility ratio is defined as the ratio of deformation at failure to deformation at yield. The advantage of the

Figure 3-1: A hysteretic damper installed in a 44-story building.

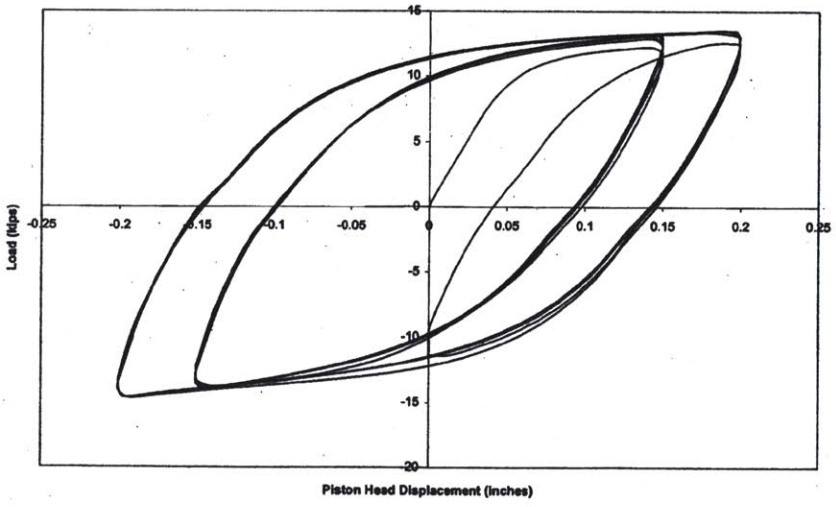

Figure 3-2: Load-deflection curves for a yielding core element.

symmetric behavior for design purposes is that the element will be using its full capacity in both tension and compression. In traditional braces, where buckling is not prevented, the member is over-designed to avoid buckling, which means it has much more tensile strength than it needs. With the buckling-restraining system however, there is no need to over-design and members will utilize their full capacity, both in tension and compression. The test results indicate another advantage of unbonded-braces, namely the well-defined elastic-plastic bilinear behavior of the member. This allows for rational capacity design methods for the members.

3.3 Recent Research on Hysteretic Dampers

As mentioned in the previous section, hysteretic dampers absorb energy through yielding. Figure 3-3 shows an idealized axial load - displacement plot for an elastic-perfectly plastic material. The energy dissipated by the mechanism is represented by the area within the curve. Hence, more energy dissipation is achieved with increasing F_y (yield strength of the material), increasing ductility ratio or decreasing u_y (displacement at yield). This realization has triggered the use of hysteretic dampers as elements that become effective at higher level of excitations (high F_y). In other words for low levels of excitation the braces simply provide stiffness for the structure, while at high levels they yield and dissipate seismic energy.

This has been the methodology used most widely so far and hence the braces that are produced by Nippon Steel, Japan, are heavy and large as can be seen in the pictures included in this chapter. These braces have a steel yielding core, inside a steel jacket with concrete filling in the gap between the two steel components. Although this system performs its structural duties well, the use of these materials results in a heavy member, necessitating the use of machinery for installation.

It can be argued that if the installation of these members were easier and less costly they would be more widely accepted by the conservative construction industry that prevails in the United States. With that in mind, KaZaK Composites Incorporated (KCI) of Woburn, MA is working on different design schemes that would result in

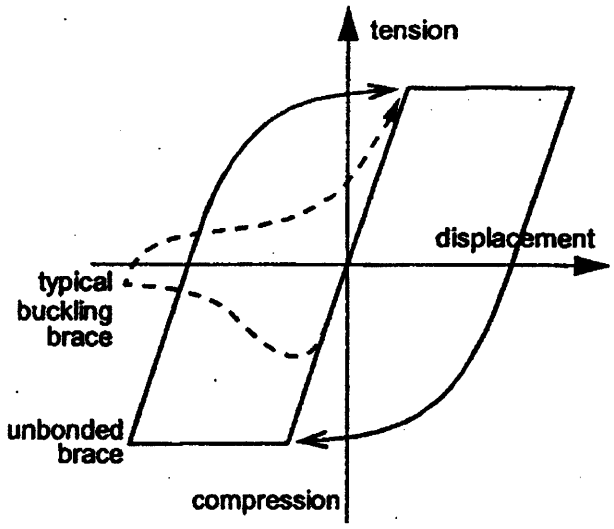

Figure 3-3: Idealized Hysteresis loop for an elastic-perfectly plastic material. Taken from [5]

lighter brace elements, such that two construction workers without any machinery help could perform their installation. Some of KCI's findings are promising and are given below. It should be stated however that the axial force capacity of the braces KCI is planning to develop will not be as high as that of the larger and heavier ones produced by Nippon Steel. Therefore the target applications for these new designs are the rehabilitations of low-rise buildings. Hence, the investigation of the uses of these new devices is very fitting for the purposes of this thesis.

To solve the problem of heavy weight, KCI proposes the of use composite materials for the anti-buckling sleeve and the spacer. Although the production cost may be higher, due to the use of composite materials, it can be argued that the savings incurred during construction will offset these extra costs. In that respect KCI investigated several options before deciding on replacing the low yield strength steel core by 1100-O annealed aluminum [2]. This selection was due to its reported 5-7 ksi yield strength and approximately 25% strain to failure. A major advantage of using 1100-O aluminum as the yielding strut material is that its weight-specific energy absorption is approximately twice that of the Nippon Steel alloy (i.e. 2/3 the yield stress at 1/3

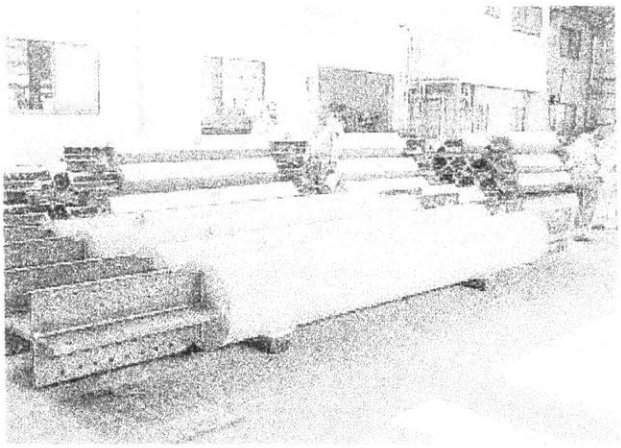

Figure 3-4: The unbonded-brace elements used in the Bennett Federal Building Project. Taken from [4]

the density). Replacing the steel buckling suppressing sleeve by a graphite/glass fiber sleeve and the concrete spacer by a foam spacer also results in weight reductions of about 70%. The resulting cross-section is shown in Figure 3-5.

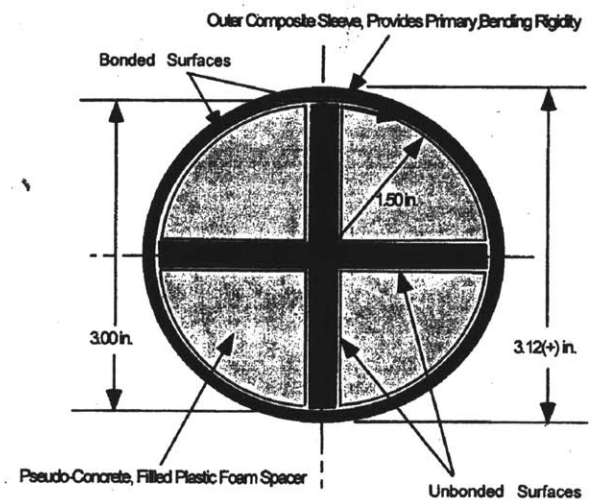

Figure 3-5: Cross-section of an hysteretic damper proposed by KCI.

As stated earlier the findings so far are promising but naturally inconclusive. There are still many aspects of the issue that are unresolved, such as the connection details between the damper and the primary structure or the marketing of the new

product. Therefore KCI is continuing the investigation and testing with the help of outside consultants.

Chapter 4

Application Studies

4.1 Building Description

This thesis concentrates on the rehabilitation of a three-story special moment resisting frame (SMRF) originally developed for a series of nonlinear time history analyses in Phase 2 of the FEMA/SAC Steel Project [5]. The building is assumed to be in Los Angeles (seismic zone 4) on stiff soil (UBC soil type S2), and was designed to meet the 1994 UBC provisions. Figure 4-1 shows the plan view of the structure along with the geometry and the member sizes of one of the moment-resisting frames in the North-South direction of the building. It should be noted that grade beams were used at the foundation level to achieve full fixity of the column bases. All the columns in the perimeter of the building bend about their strong axes, which are oriented in the North-South direction. Further details of the building can be found in Appendix B of Reference [3].

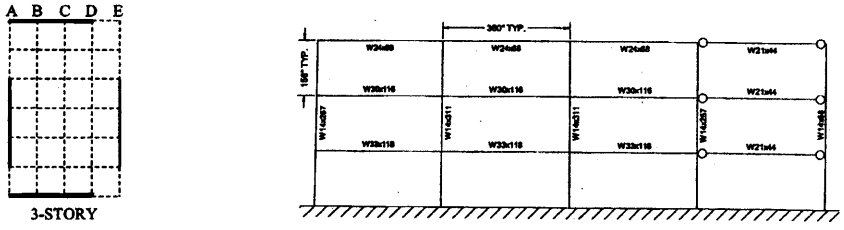

Figure 4-1: Floorplan and elevation views of the original structure. Taken from [3] and [5].

The designs of the moment frames are almost identical in the two orthogonal directions, therefore only half of the structure is analyzed. Also, the difference between the North-South (NS) and East-West (EW) is due to the difference in gravity load effects caused by the beams and sub-beams, since they are both oriented in the NS direction. However, because these load effects are negligible in moment frames, the analysis of the structure can safely be reduced to the analysis of only the NS direction. Since only half of the structure is being analyzed the seismic masses, given as per floor values, were divided by two to obtain the values given in Table 4.1.

Table 4.1: The mass of each story

Story	mass(kips-sec^2/ft)	mass(kg)
1	32.77	478,560
2	32.77	478,560
3	35.45	517,780

In accordance with the Rehabilitation Objective selected for this study, under BSE-1 excitation the primary structure is to remain in the elastic range and have a maximum drift of 0.5%, which corresponds to a maximum allowable shear strain of $\gamma_{max} = 1/200$. Considering the height each floor the following design criteria are obtained:

Maximum drift at the top, $u_3^* = 0.195$ ft (0.06m)

Maximum allowable interstory drift, $\Delta u^* = 0.065$ ft (0.02m)

In what follows, three different design methodologies will be introduced and walked through step-by-step. Then these methods will be compared to each other in an attempt to identify the optimal one.

4.2 Strength Based Design

As mentioned in the Chapter 1, Strength Based Design is the design philosophy used in the current building codes. In order to understand the merits and disadvantages

of the alternative design methodologies this thesis proposes, one needs to attain an understanding of how Strength Based Design is performed and how the final structure behaves under the specified loads. In that respect, the building introduced in Section 4.1 is designed here according to the Uniform Building Code (UBC). However, chevron bracing is used to provide lateral stiffness, replacing the moment carrying frame system.

The strategy offered by UBC is to apply a quasi-static inertia force that is equivalent of an earthquake loading. The building is modeled as a simple beam with masses lumped at story heights, where these inertia forces are applied (see Figure 4-2). The shear caused by these inertia forces are then computed per floor along with the necessary stiffness to prevent extreme deformation. The cross-sectional areas of the bracing elements is calculated by taking into account the geometry (of the chevron brace) and by assuming the brace is acting at the yield stress. The latter is a code criteria for eccentric braced frames.

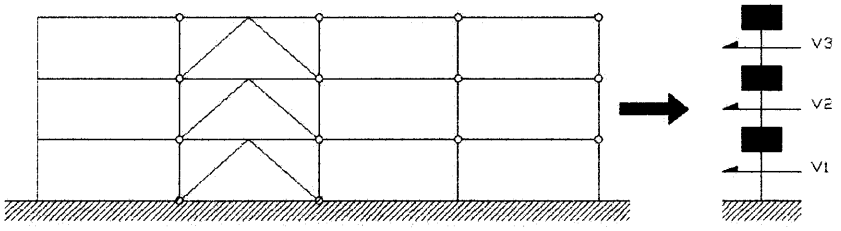

Figure 4-2: The lumped-mass model of the original building with shear forces.

The shear force experienced by the first floor (base shear) is given as $V_1 = 0.099W$, where W is the weight of the building. The base shear is proportioned and applied at each floor according to the weight of the stories above that particular floor. The obtained shear forces are increased by 50% as required by allowable stress design to obtain the following values:

$V_1 = 483$ kips

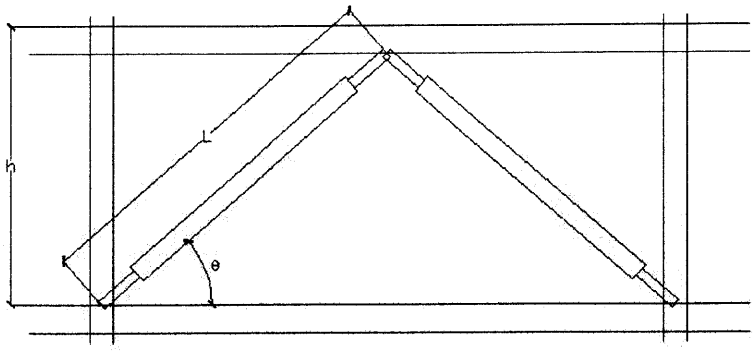

Figure 4-3: The chevron brace configuration used for the stiffness and hysteretic damper installations.

$V_2 = 326$ kips

$V_3 = 170$ kips

Following the design in Reference [5] the yield strength of the braces is taken as 34 ksi and is further reduced by 10%. Assuming the brace element acts at the yield stress, the area of each brace element is simply:

$$A_i = \frac{F_i}{0.9\sigma_y} \tag{4.1}$$

where, F_i is the force each brace element experiences due to the shear on floor i. Taking θ as the angle the brace makes with the horizontal(see Figure 4-3), and remembering that there are two braces per floor, the force in each element is given by:

$$F_i = \frac{V_i}{2cos\theta} = \frac{V_i}{1.31} \tag{4.2}$$

These definitions yield to the following values of area for each brace element:

$A_1 = 12.05$ in^2

$A_2 = 8.14$ in^2

$A_3 = 4.23$ in^2

In order to see the response of the structure under certain seismic loads, the stiffness per floor was calculated using Equation 4.3.

$$k_i = 2\left(\frac{AE}{L}\right)_i cos^2\theta_i \tag{4.3}$$

The resulting stiffness values were then entered into MotionLab[1] No damping was assigned to the structure in this analysis as the design procedure followed in this section does not incorporate any damping. The low damping (i.e. 1–2%) provided by the structural frame is ignored.

$$k_1 = 1258 \text{ kip/in}^2 \quad = 220 \text{ MN/m}^2$$

$$k_2 = 850 \text{ kip/in}^2 \quad = 149 \text{ MN/m}^2$$

$$k_3 = 442 \text{ kip/in}^2 \quad = 77.4 \text{ MN/m}^2$$

The displacement results from MotionLab indicated that the structure had deformed more than the allowable limit defined in Section 4.1. The maximum displacement observed on the third floor was $u_3 = 0.43$ m, while the interstory displacement was $\Delta u = 0.15$ m.

4.3 Design with Hysteretic Dampers: Method 1

As the first step, the building is modeled as a discrete shear beam with lumped masses (as calculated in Section 4.1) at story heights and varying lateral stiffness for each floor. The stiffness per floor was calculated using the following equations:
For interior columns:

$$k_{int} = \frac{12EI_c}{h^3(1+r)} \tag{4.4}$$

For exterior columns:

$$k_{ext} = \frac{12EI_c}{h^3(1+2r)} \tag{4.5}$$

[1]MotionLab is a computer analysis software developed by J. J Connor. It analyzes lumped mass models (in the linear region) using conventional or modal state-space formulations. It allows the analyst to enter different values of mass, stiffness and damping values for each story.

where,

h : floor height

$r = \frac{I_c}{h}\frac{L_b}{I_b}$

E : Modulus of Elasticity

I_c : Moment of Inertia of the column

I_b : Moment of Inertia of the beam

L_b : Length of the beam

The calculations in Appendix B result in the following stiffness values:

k_1 = 465 kip/in (81,440 kN/m)

k_2 = 411 kip/in (72,030 kN/m)

k_3 = 188 kip/in (32,920 kN/m)

It should be mentioned that the bending deformation effects were neglected in these calculations since experience shows that low-rise buildings such as the one under investigation show a shear-beam response as opposed to a bending-beam response [6].

The modal shape observed when the original structure was subjected to BSE-1 excitation is given in Figure 4-4. Note that the modal shape gives relative values of displacement, not absolute, as the displacement of each node is normalized with respect to the maximum nodal displacement. Although the modal shape is close enough to the desired modal shape (i.e. constant interstory displacement) for the first mode the magnitude of the displacements, given below, are much higher than the design limits specified Section 2.2. These two findings were the basis for attempting to the bring the response of the building down to acceptable limits by applying damping to the system, without increasing the stiffness.

u_3 = 0.75m (29.53in) $\quad$ Δu = 0.25m (9.84in)

T_1 = 1.23sec $\quad$ T_2 = 0.52sec $\quad$ T_3 = 0.30sec

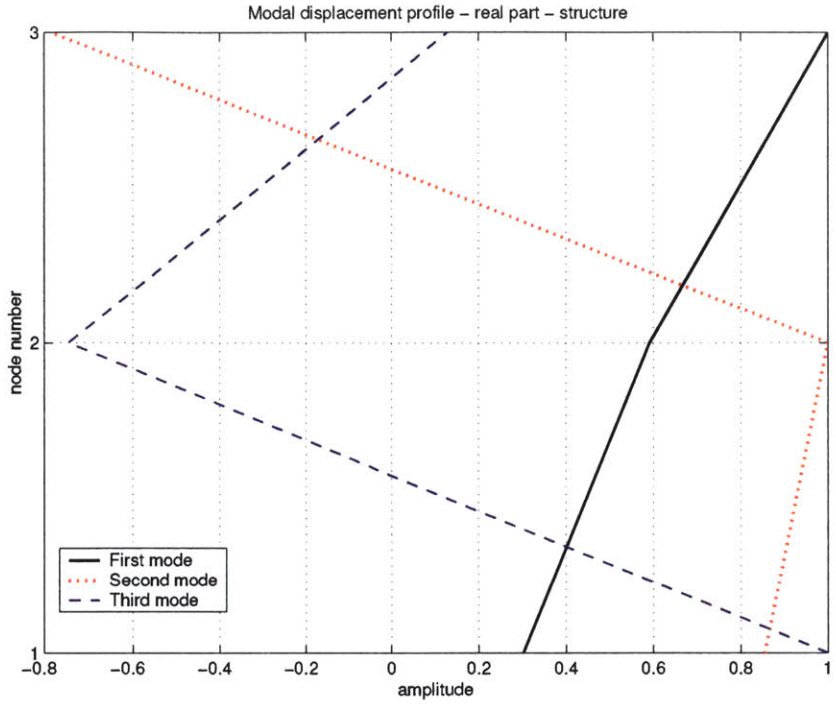

Figure 4-4: The modal shape of the original structure subjected to BSE-1.

Many simulations were run with various values of c_{av} (the damping coefficient per floor) with the objective of reducing the response. Results of some of the runs are tabulated in Table 4.2. These results indicate that additional damping causes considerable increase in the damping of the second and third modes, while, the modal damping for the first mode is not as sensitive to the changes in the c_{av} value.

Around c_{av}=5 500 000 Ns/m an interesting phenomenon was observed. The modal periods and modal displacement profiles changed orders. As the value of the damping coefficient was increased even further the second mode became overdamped and the period of the second mode jumped up to around 600 seconds, which suggested that the solution blew up and should be discarded. This unexpected phenomena is worth investigating in greater detail. However, as it did not fit into the scope of this thesis, the problem was avoided by selecting c_{av} values that were smaller than the limiting value.

Table 4.2: Results of runs 1-6.

Run#	c_{av}(MN-s/m)	ξ_1(%)	ξ_2(%)	ξ_3(%)	T_1(s)	T_2(s)	T_3(s)	u_3(m)	Δu(m)
1	1.50	7.0	21.5	23.0	1.23	0.53	0.31	0.260	0.087
2	2.50	11.5	36.0	38.5	1.23	0.55	0.32	0.200	0.067
3	3.50	15.5	51.0	54.0	1.23	0.57	0.33	0.175	0.058
4	4.50	20.0	67.0	71.5	1.23	0.65	0.47	0.157	0.052
5	5.00	22.0	74.0	81.0	1.23	0.69	0.58	0.157	0.052
6	5.45	23.0	94.0	77.0	1.23	1.12	0.67	0.144	0.048

Change in Strategy

The initial strategy was to increase damping while keeping the stiffness constant until the response of the structure was decreased to the allowable values. The value of damping at which the structure's response was within the allowable values was going to be taken as the upper limit for damping.

However, the phenomenon observed around c_{av} = 5 500 000 Ns/m lead to a modification of the strategy. Damping coefficient of 5 450 000 Ns/m was taken as the upper limit for damping and the stiffness values of each floor were adjusted. It should be noted however, that the value of 5 450 000 Ns/m was the limiting value for the damping coefficient, for the structure with no additional stiffness. As more stiffness was added to the structure, the value of 5 450 000 Ns/m for damping was no longer a limiting value and the overdamping of the second mode was avoided. The modified strategy is as follows:

1. For the first run, enter the original stiffness values (i.e. the stiffness of the original building, k_i's used in Runs 1-6) as the initial stiffness values, however utilize the "iterate on stiffness" option of MotionLab [2]. As for the damping coefficient value, use the upper limit value of c_{av} = 5 450 000 Ns/m.

2. Record the displacement results.

3. For the subsequent runs, enter the original stiffness values as the initial stiffness

[2]The algorithm MotionLab follows consists of iterating on the stiffness values on a per floor basis until the displacements obtained are less than the design value. The outline of the algorithm can be found in Chapter 2 of [6].

values and click on the "iterate on stiffness" option, just like in Step 1. However, pick different c_{av} values depending on the results from the previous run.

4. Record the displacement values and repeat Step 3 as many times as necessary, until the displacements converge on the design values.

The results of the runs following this procedure are listed in Table 4.3.

The results of Run 7 show that the structure's response is under the maximum allowable deformation. However, the values are considerably lower than the design values, suggesting the existence of a more efficient design (i.e. a stiffness and damping combination) that yields a response that is closer to the desired response. Just like in any design, an iterative process is followed after Run 7 by changing the damping values to obtain a response that is as close to the design response as possible.

Table 4.3: Results of Runs 7-10.

Run	k_1 (MN/m)	k_2 (MN/m)	k_3 (MN/m)	c_{av} (MN-s/m)	ξ_1 (%)	ξ_2 (%)	ξ_3 (%)	u_3 (m)	Δu (m)
7	920	690	410	5.45	7.0	22.5	26.5	0.049	0.016
8	720	520	280	9.50	15.0	48.0	53.0	0.053	0.018
9	660	480	250	11.5	19.0	62.0	68.0	0.058	0.019
10	650	480	240	12.5	21.0	68.5	26.0	0.058	0.019

Since the structure was "too stiff" in Run 7 a higher damping coefficient value (c_{av}=9 500 000 N-s/m) is used in the next run, leading to smaller iterated stiffness values. The resulting displacement values are once again considerably lower than the design values, hence value of the damping coefficient is increased once more to c_{av}= 11 500 000 N-s/m in Run 9.

The results of Run 9 are "pretty good" and most likely adequate for preliminary designs. However, an additional run was completed as a way to check that the results really are converging on the design values. Although the displacement values obtained from Run 10 were indeed closer to the design values, the difference was negligible. It needs to be mentioned here that the controlling value for the iterations performed on the stiffness values is the interstory displacement. The iterations continue until

the average of the interstory displacements is equal to the design value, which in this case is 0.02m. If this happens to be an unsatisfactory or an inappropriate controlling criteria, then one can use the stiffness values from the previous run, modify them slightly and run a new analysis without iterations.

The results of Run 10 also indicate that increasing the damping coefficient to 12 500 000 N-s/m (8.6% increase) caused only a negligible decrease (1.4%) in the total required stiffness of the building. This may be an important factor to consider for design since the magnitude of total stiffness and damping are related to the cost. This issue will be discussed in more detail in Chapter 6.

An additional factor that may be of importance is the number of iterations performed on the stiffness values for each run. Table 4.4 shows how many iterations were required to achieve the desired interstory displacement for each run. As one might imagine, the more the iterations, the higher the cost of calculations, especially for larger projects.

Table 4.4: Number of iterations required for Runs 7-10.

Run	# of Iterations
7	3
8	4
9	6
10	8

4.3.1 Conclusion

The results of this analysis shows that the original structure is extremely vulnerable to BSE-1 earthquake and that its stiffness is about a magnitude smaller than what it should be for the deformations to be acceptable. This confirms that moment frame systems do not provide much lateral stiffness, even when hefty members are used. In addition to being a moment frame, the relatively long bay widths, also caused the effective lateral stiffness to be small for this particular building.

Most of the work involved in this method was about finding approximate values

for the optimal damping and stiffness values. Additional and sometimes considerable number of iterations were necessary afterwards for fine-tuning the response.

4.4 Design with Hysteretic Dampers: Motion Based Design Approach

The design approach followed in Section 4.3 consisted of increasing the stiffness of the original building and adding damping to it until the desired response was achieved.

One can however, take a different approach to obtain close estimates to the stiffness and damping values directly. This method, which is explained below, is taken from [6] and is named the Motion Based Design (MBD) approach. Similar to the previous method, once the approximate values of optimal stiffness and damping are obtained, fine-tuning is necessary.

The starting point is the equilibrium equation for a damped system:

$$\mathbf{M}\Phi^*\ddot{q} + \mathbf{C}\Phi^*\dot{q} + \mathbf{K}\Phi^* q = \mathbf{P} \tag{4.6}$$

where, q is the displacement variable and the mass, $\mathbf{M}$ and the stiffness, $\mathbf{K}$, matrices are given as:

$$\mathbf{M} = \begin{bmatrix} m_1 & 0 & 0 \\ 0 & m_2 & 0 \\ 0 & 0 & m_3 \end{bmatrix}, \qquad \mathbf{K} = \begin{bmatrix} k_1 + k_2 & -k_2 & 0 \\ -k_2 & k_2 + k_3 & -k_3 \\ 0 & -k_3 & k_3 \end{bmatrix} \tag{4.7}$$

where the subscripts denote the story number.

The $\mathbf{\Phi^*}$ matrix is the desired modal shape. Since the desired modal shape for mode 1 corresponds to a constant interstory displacement, $\mathbf{\Phi^*}$ is given as:

$$\mathbf{\Phi^*} = \begin{pmatrix} 1/3 \\ 2/3 \\ 1 \end{pmatrix} \tag{4.8}$$

The construction of the damping matrix, $\mathbf{C}$ depends on how the designer wishes to vary the damping throughout the structure. In this study, damping is distributed uniformly between the three floors, i.e. every floor has the same damping coefficient, c_{av}. For this type of damping distribution the $\mathbf{C}$ matrix has the same form as the $\mathbf{K}$ matrix:

$$\mathbf{C} = \begin{bmatrix} c_1 + c_2 & -c_2 & 0 \\ -c_2 & c_2 + c_3 & -c_3 \\ 0 & -c_3 & c_3 \end{bmatrix} = \begin{bmatrix} 2c_{av} & -c_{av} & 0 \\ -c_{av} & 2c_{av} & -c_{av} \\ 0 & -c_{av} & c_{av} \end{bmatrix} \tag{4.9}$$

Since in seismic excitations the nodal forces are proportional to the nodal masses, the force matrix, $\mathbf{P}$ is defined as:

$$\mathbf{P} = -a_g \begin{pmatrix} m_1 \\ m_2 \\ m_3 \end{pmatrix} \tag{4.10}$$

where m_i are the floor masses and a_g is the ground acceleration.

Multiplying Equation 4.6 by $(\Phi^*)^T$ yields:

$$\tilde{m}\ddot{q} + \tilde{c}\dot{q} + \tilde{k}q = \tilde{p} \tag{4.11}$$

where the quantities with superscript tilde are equivalent one degree of freedom mass, damping, stiffness and force quantities. They are defined and calculated as:

$$\tilde{m} = (\mathbf{\Phi^*})^{\mathbf{T}}\mathbf{M}\mathbf{\Phi^*} = 7.836 \times 10^5 \text{kg} \tag{4.12}$$

$$\tilde{c} = (\mathbf{\Phi^*})^{\mathbf{T}}\mathbf{C}\mathbf{\Phi^*} = 2\tilde{\xi}\omega\tilde{m} \tag{4.13}$$

$$\tilde{k} = \omega^2\tilde{m} \tag{4.14}$$

$$\tilde{p} = (\mathbf{\Phi^*})^{\mathbf{T}}\mathbf{P} \tag{4.15}$$

$\tilde{p}$ is usually expressed in terms of the equivalent mass, $\tilde{m}$ and the modal participation factor, Γ, as:

$$\tilde{p} = -\Gamma\tilde{m}a_g \tag{4.16}$$

where,

$$\Gamma = \frac{\sum m_i \Phi_i}{\tilde{m}} = 1.271 \tag{4.17}$$

Using these definitions and results, the stiffness for each floor is obtained. During the process one utilizes the response spectra shown in Figure 4-5. Since the maximum

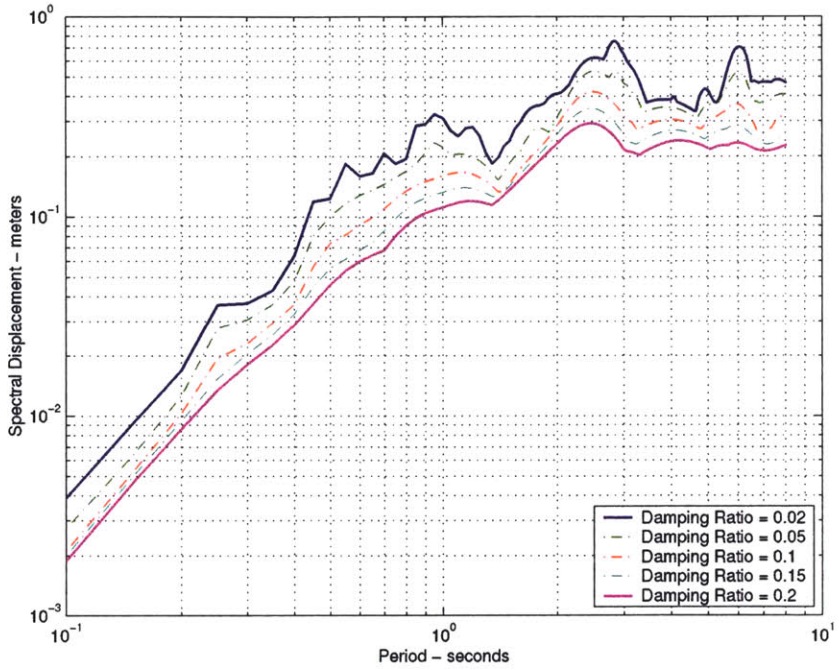

Figure 4-5: Response Spectra for BSE-1.

allowable maximum displacement is $u_3^* = 0.06$m at the top, from the response spectra, one can obtain what the period of the structure should be by assuming a damping ratio for the system. However, since response spectra plots are for SDOF systems, one uses the modal participation factor Γ to express the current 3-DOF problem as a SDOF problem. Hence, the design spectral displacement is:

$$S_d^* = \frac{1}{\Gamma} u_3^* = 0.0467\text{m} \tag{4.18}$$

In this study the stiffness calibration was based on a damping ratio of, ξ= 20%. This damping ratio along with the maximum allowable shear deformation lead to a struc-

ture with a period of T = 0.50 seconds (from Figure 4-5). The stiffness distribution that yields that period value is:

$$k = \begin{pmatrix} 472 \\ 396 \\ 245 \end{pmatrix} \times 10^6 \text{N/m} \tag{4.19}$$

The damping coefficient per floor is obtained by:

$$\tilde{c} = 2\xi\omega\tilde{m} = \frac{1}{3}c_{av} \tag{4.20}$$

$$c_{av} = 11.8 \times 10^6 \text{N-s/m} \tag{4.21}$$

These values of stiffness and damping should theoretically yield a response that is equal to the design limit. As a check these values are entered into MotionLab, the response is observed and modifications are made in a fashion similar to the method of Section 4.3. Results of these runs, Runs 101-106 are listed in Table 4.5.

Table 4.5: Results of Runs 101-106.

Run	k_1 (MN/m)	k_2 (MN/m)	k_3 (MN/m)	c_{av} (MN-s/m)	ξ_1 (%)	ξ_2 (%)	ξ_3 (%)	u_3 (m)	Δu (m)
101	472	397	245	11.8	20.0	62.0	81.0	0.078	0.026
102	472	397	245	13.0	22.0	90.0	68.0	0.075	0.025
103	700	510	360	13.0	22.0	67.0	77.0	0.052	0.017
104	650	500	330	13.0	19.0	58.5	77.0	0.052	0.017
105	550	450	330	13.0	20.0	59.0	82.0	0.062	0.021
106	570	440	330	13.0	20.0	83.0	58.0	0.060	0.020

During Runs 101-103 the limiting value for the damping coefficient was found to be c_{av}=13 000 000 N-s/m. On Run 103, the iteration function was selected, so that the stiffness values would be iterated until an interstory displacement of $\Delta u = 0.020$m is obtained. However, results of Run 103 and some intermediate runs that are not given here, showed that the iterations caused the building to be too stiff. Therefore in Runs 104 to 106 manual iterations were performed based on the result of the previous run, until the desired response was achieved.

4.4.1 Conclusion

In the MBD approach stiffness and damping values that yield approximately the design deformations are obtained initially following a simple algorithm introduced above. Then, several manual "iterations" are necessary to achieve the design criteria. The main difference between MBD approach and approach of Method 1 is the amount of flexibility (and hence responsibility) given to the designer. The designer needs to be able to interpret the results of a run properly in order to make the necessary modifications on certain parameters for the next run. In addition, the number of iterations required in Run 103 was only one. Attaining an approximate value for stiffness using the MBD approach required less iterations. Again this may have significant impact on the cost of the calculations for larger scale projects.

Chapter 5

SAP Analyses

5.1 Introduction

In Chapter 4, three design methodologies were presented, one being the more traditional Strength Based Design. The latter two methodologies are associated with damage controlled design and introduce stiffness and damping to the structural system. In this chapter the optimal design values obtained in Chapter 4 will be input into SAP2000[1] to observe the structure's response under BSE-1 and BSE-2 loadings. Since the Performance Level to be used for design purposes allows the structure to enter the nonlinear region under BSE-2 loading, the use of SAP2000 Nonlinear was necessary.

It was previously shown, in Section 4.2 that the structure resulting from the Strength Based Design would experience unacceptable deformations even under BSE-1 loading. Therefore, that design approach is discarded. Although the remaining two methods were very similar in nature the results of the Motion Based Design Approach will be used here simply because it is the approach that provided the designer with more flexibility and responsibility during the process.

[1] A widely used finite element structural analysis program produced by Computers & Structures, Inc.

5.2 Input

The first step in the SAP2000 analysis was to enter the geometry of the building and then to assign sections to the frame members in accordance with the original building. After this was completed the two loading Time History Functions and Cases were defined for the BSE-1 and BSE-2 excitations.

Then the retrofit began, i.e. the additional stiffness and dampers were installed using the chevron brace configuration. Both the braces that provide the stiffness and the damping elements were defined as NonLinearLink (NLLink) elements, as discussed in the next section. For analysis purposes that the dampers and the main lateral stiffness members were placed in different bays for reasons of clarity[2]. During actual construction the location of these elements would be governed by other factors, such as accidental torsion effects. It should be noted however, there is no reason for the dampers not to be put in the same bay as the braces that provide stiffness. How the necessary properties for the stiffness and damper members were obtained and entered into SAP2000 are explained next.

5.2.1 Assigning the "optimal" stiffness and damping values

From the results of the Motion Based Design approach required stiffness and damping values per floor are given as:

$$k_1 = 570 \text{ MN/m} = 3255 \text{ kip/in}$$

$$k_2 = 440 \text{ MN m} = 2512 \text{ kip/in}$$

$$k_3 = 330 \text{ MN/m} = 1884 \text{ kip/in}$$

The first thought that comes to mind is to provide the total floor stiffness by the brace elements, which are the traditional braces using normal 36ksi steel, and add the dampers totally separately. The dampers themselves would be providing some lateral

[2]The analyses were performed using only a two bay structure, rather than the four bay structure. This simplification could be made, since eliminating the additional stiffness provided by the bending of the members in the other bays lead to a more conservative analysis.

stiffness, however that value could be kept to a negligible magnitude by adjusting the length of the yielding core element since the stiffness is given by:

$$k = \frac{AE}{L}$$

where L is the length of the yielding element.

However, the analysis of the structure revealed that the damping mechanism was not functioning at all. The time history plot in Figure 5-1 clearly shows there is practically no force taken by the damper elements. This was confirmed when the response was checked and found to be close to that obtained in the case with no damping. Although, surprising and discouraging at first, these results were justified and rationalized shortly after. Load will always follow the path of most stiffness to find its way to the foundations. Since all of the stiffness in the structure is provided by the brace elements, all of the lateral load is resisted by them as well, leaving negligible forces to be experienced by the dampers. The magnitude of the forces the dampers experienced were not large enough to cause the necessary yielding for damping to take effect.

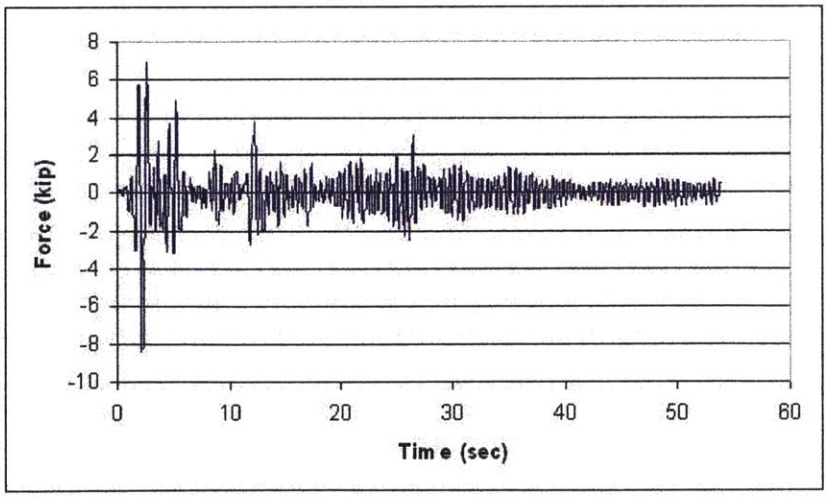

Figure 5-1: The force experienced by the dampers is negligible, considering the dampers have a yield strength of 386.4 kips

This realization lead to a solution in which the required lateral stiffness per floor was divided between the dampers (k_d) and the braces (k_b). How one would design the elements to achieve these values in real life is discussed in the following sections. A more complicated issue is determining the optimal distribution of the total story stiffness (k_s) between the dampers and the braces. The distribution should be done such that the dampers "draw" enough force to yield as many times as possible during the excitation. However, the distribution should also be such that,

$$\frac{k_d}{k_b} \leq 1$$

This criteria ensures that the stiffness provided by the dampers is at most equal to that provided by the braces. Ideally this ratio should be as small as possible, because hysteretic damper elements are designed to be replaced every so often[3] and it is not desirable for the structure to lose a significant amount of its lateral resistance during the replacement process. Depending on the owner's and/or the designer's wishes, this criteria could be made more stringent.

The theoretical method to arrive at the correct distribution of the story stiffness, k_s, and why that methodology was deemed inappropriate is discussed in the following sections. As an alternative to the theoretical approach, numerical simulations were run using SAP2000 with varying parameters to attain relationships that can be used to determine the ideal stiffness distribution.

As mentioned in Section 5.2, both the stiffness braces and the dampers are modeled as NLLink members in SAP2000, because it is expected that especially under BSE-2 both mechanisms may go into the plastic region. The Plastic type NLLink elements in SAP2000 are those that have an initial stiffness until yielding and a reduced, secondary stiffness post-yielding. As such, this type of NLLink elements are deemed to be most appropriate to model both the braces and the dampers. Figure 3-3 shows

[3]These elements can only take up to a certain number of cycles, after which they become ineffective. The number of cycles until that stage is reached varies with many factors and is a design parameter that needs to be considered. For the purposes of this study, it is adequate to say that the hysteretic dampers are designed to be replaced

the idealized Force-deformation curve for a elastic-perfectly plastic[4] material.

Figure 5-2 shows the dialog box one uses to enter the properties of a plastic NLLink element. There are two sections to fill in this dialog box; Linear Properties and NonLinear Properties. The Effective Stiffness and the Stiffness values in these sections refer to the same parameter, and should be assigned the value of the stiffness of the member in the elastic region. Effective damping box is not applicable to neither the hysteretic dampers nor the stiffening braces, hence value of zero should be assigned. The yield strength is the magnitude of the force required to yield the element. The Post Yield Stiffness Ratio is the ratio of the post yield stiffness to stiffness (or effective stiffness). Since both elements are idealized as elastic-perfectly plastic this ratio is taken as zero as well[5]. The yielding exponent is kept at its default value of 2.

The two parameters one can utilize to attain the optimal stiffness distribution are the stiffness and the yield strength for both the dampers and the braces. To see how the response of the structure was related to these two parameters a total of 12 runs were performed. In these runs the stiffness distributions were:

Runs 1-4: $k_d = 50\%\ k_s$ and $k_b = 50\%\ k_s$

Runs 5-8: $k_d = 30\%\ k_s$ and $k_b = 70\%\ k_s$

Runs 9-12: $k_d = 10\%\ k_s$ and $k_b = 90\%\ k_s$

The stiffness distribution schemes are named as 50-50, 30-70 and 10-90, where the first number specifies the percentage of story stiffness provided by the dampers and the second number specifies the percentage of stiffness provided by the braces. For instance in Runs 5-8, 70% of the total desired story stiffness, (see beginning of Section 5.2.1) is to be provided by the brace elements. Hence their cross-sectional areas

[4]Perfectly plastic means post-yield stiffness is zero

[5]A very small value such as 0.0001 is used for analysis purposes, because entering zero creates instabilities in the structure

are designed to give the following stiffness values per floor.

$$k_b^1 = 70\%(3255) \text{ kip/in} = 2279 \text{ kip/in} \tag{5.1}$$
$$k_b^2 = 70\%(2512) \text{ kip/in} = 1758 \text{ kip/in}$$
$$k_b^3 = 70\%(1884) \text{ kip/in} = 1319 \text{ kip/in}$$

Each stiffness distribution lead to new values of yield strength for the braces, which was calculated by the following formulas:

$$A_b^i = k_s^i \frac{L}{2Ecos^2\theta} \tag{5.2}$$
$$F_{b_y}^i = A_b^i \sigma_{b_y}^i \tag{5.3}$$

where superscript i denotes the story number, subscript y stands for "yield", L is the length of the brace element, and θ is the angle the brace element makes with the horizontal.

For each stiffness distribution 4 values of damper yield strengths were considered to vary the effective damping and observe the effect on the response of the structure. These values correspond to a maximum value of F_{d_y}= 368.4 kips and fractions of that maximum value. Selection of F_{d_y}= 368.4 kips is justified in Section 5.4. Note that the same yield strength is used for all floors, since this parameter is kept constant throughout the building in this analysis.

5.3 Results and Interpretation

Table 5.1 provides the maximum displacement observed at the top floor for BSE-1 and BSE-2 excitations for these 12 runs.

Figures 5-3 – 5-5 show how the response of the structure varies with the yield strength of the dampers and how it relates to the design displacements for BSE-1 and BSE-2 (shown as thick horizontal lines). Here are some of the conclusions that can

Table 5.1: Results of Runs 1-12.

Run	Stiffness Distribution	F_{d_y} (kip)	u_{3max} (in) BSE-1	u_{3max} (in) BSE-2	drift (%) BSE-1	drift (%) BSE-2
1	50 – 50	368.4	6.532	10.61	1.40	2.27
2		184.2	7.302	11.37	1.56	2.43
3		122.8	7.385	11.56	1.58	2.47
4		92.10	7.720	11.83	1.65	2.53
5	30 – 70	368.4	4.273	8.045	0.91	1.72
6		184.2	5.217	9.130	1.11	1.95
7		122.8	5.740	9.875	1.23	2.11
8		92.10	6.050	10.18	1.29	2.18
9	10 – 90	368.4	5.473	6.537	1.17	1.40
10		184.2	4.283	7.134	1.12	1.46
11		122.8	5.224	6.847	0.92	1.52
12		92.10	5.036	7.356	1.08	1.57

be drawn from these graphs:

1. The 10-90 stiffness distribution results in the least displacement on the third floor for both earthquake excitations. However, this is not necessarily due to a more effective damping mechanism. In fact, due to the lower stiffness provided by the dampers, the time history plots indicate that there is less yielding occurring, leading to lower effective damping. The response of the structure is therefore governed by the stiffness and not the damping.

2. Within each stiffness distribution scheme, increasing the yield strength of the dampers leads to less displacement of the third floor[6]. For this particular structure, the response is governed by stiffness and not damping, which means an increase in stiffness is more effective than the same amount of increase in damping. Since increasing the yield strength of the dampers leads to more elastic behavior (and more stiffness), the displacements observed are lower for higher yield strength values.

3. Even if more yielding is achieved by decreasing the yield strength of the material, the effective damping may still be lower. Recalling the idealized Force-

[6]Except for the local dip observed in the 10-90 stiffness distribution case.

deformation plot in Figure 3-3, it can be seen that less energy dissipation (i.e. less area inside the curve) is achieved with decreasing yield strength. Hence the optimal yield strength is a function of the interaction of these two phenomena: Amount of yielding and size of the Hysteresis loop.

4. None of the stiffness distribution and yield strength combinations resulted in a structure that satisfied the displacement criteria for BSE-1. This is surprising since, previous analyses in Chapter 4 had shown that certain combinations of stiffness and damping per floor would result in a satisfactory design. The reason, for the discrepancy between two analyses has to do with how hysteretic damping is modeled as an equivalent viscous damping and is discussed further in Section 5.4.

5. It is possible to achieve a response that satisfies the design criteria for BSE-2 excitation. This is partially due to an increase in the effectiveness of the hysteretic dampers for larger excitations.

Concluding that the structure's response is dominated by stiffness has significant consequences. It suggests that damping does not contribute significantly to the design, and the best design consists of stiffness only (i.e. no damping). Section 5.4 attempts to explain the reasons for this and other unexpected results of these runs.

5.4 What Went Wrong?

As mentioned earlier, analyses performed by MotionLab and discussed in Chapter 4 suggested that damping had a significant effect on the response of the building. However, in the previous section it is concluded that stiffness is the only important factor. What is the reason for this paradox?

5.4.1 Expressing Hysteretic Damping as Equivalent Viscous Damping

In fact there is no paradox. The conclusion drawn in the previous section is only true for hysteretic dampers. The root of the problem lies in the expression used to convert hysteretic dampers into equivalent viscous dampers. The conversion formula, Equation 5.4[7], holds true if the excitation is periodic with an amplitude $\bar{u}$ and frequency Ω and if in every cycle the material yields.

$$F_y = \frac{\pi \Omega \bar{u}}{4} \left(\frac{\mu}{\mu - 1} \right) c_{av} \tag{5.4}$$

where μ is the ductility ratio, defined as the ratio of the maximum extension of the member to the extension at which the member yields.

Figures ?? and ?? show the Time Histories of the forces the hysteretic damping elements in the first story experience. The dampers were given a yield strength of 122.8 kip in this particular case. A careful examination of the plot shows that the dampers reach the yielding point many more times for the BSE-2 excitation, hence making the effective damping larger for that case. In fact, if the excitation was so large that the elements yielded at every cycle, Equation 5.4 would work almost[8] perfectly.

In other words, Equation 5.4 represents the ideal case in which the energy dissipation is maximized. When the correct value are given to the parameters in that equation, the yield strength one obtains is 368.4 kips. That is why that value was taken as the maximum value for the yield strength of the hysteretic dampers. A value more than that would result in no yielding for some of the cycles in the loading, which corresponds to linear behavior and no energy dissipation hence less effective damping (i.e. no area within the Force-displacement curve).

This also justifies the attempts to increase the effective damping by decreasing the yield strength of the dampers. When one looks at Equation 5.4, it is clear that

[7] This formula is based on equating the energy dissipated per cycle of excitation to that of a linear viscous damper.

[8] "Almost" because the frequency of the excitation is not constant and the natural frequency of the structure is used to replace Ω in Equation 5.4

taking a smaller value for $\bar{u}$ would mean a smaller value for F_{d_y} and therefore allow the elements to yield earlier and more frequently, ideally every cycle, during the excitation. However, as mentioned earlier, whether decreasing the yield strength of the member achieves more effective damping depends on an additional factor. Since energy dissipation per cycle is given by the area within the Force-deformation curve (see Figure 3-3), there is a limit as to how low the yield strength should be.

5.4.2 The Earthquake

The design earthquake chosen for this study was the Imperial Valley 1940 earthquake, because it is a representative earthquake for the Mid-California region; the region that is of most interest in the United States. As the time history of the ground acceleration in Figure 2-3 shows, this earthquake shows an impulsive behavior, meaning that it reaches its peak ground acceleration (PGA) of 134.5 in/sec^2 (3.42 m/sec^2) very early on and doesn't get close to that maximum value many times after that. It is not hard to see that this type of earthquake is probably the farthest one away from a periodic loading, for which Equation 5.4 holds. A study with a larger variety of earthquakes would yield more acceptable and reliable results.

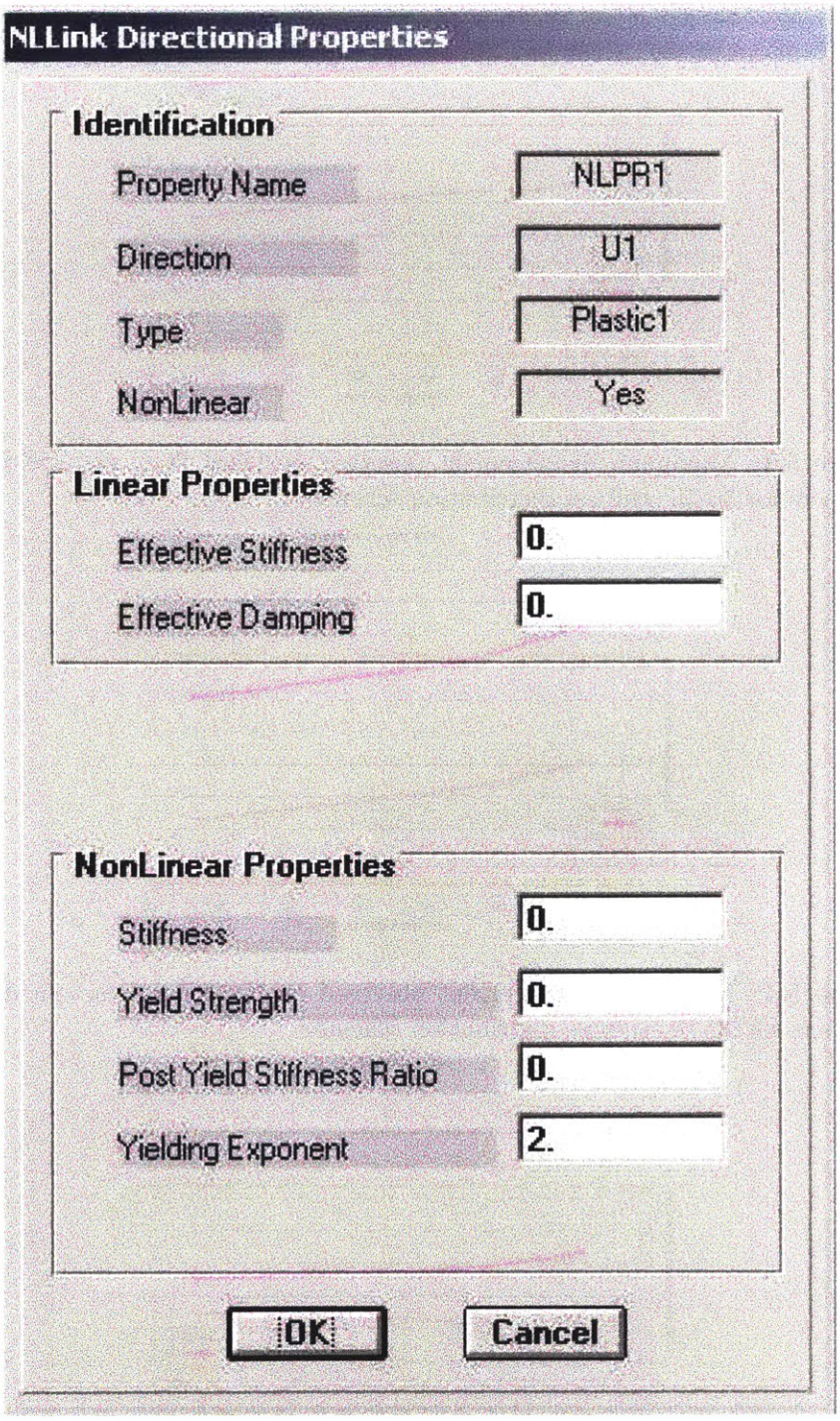

Figure 5-2: The dialog box in SAP2000 where the properties of NLLink elements are defined.

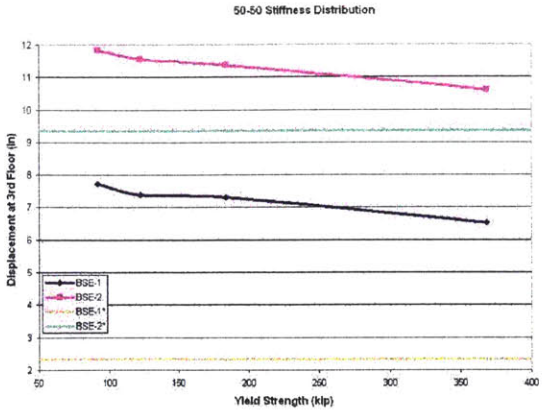

Figure 5-3: Maximum displacement observed on third floor vs. yield strength of dampers for 50-50 stiffness distribution scheme.

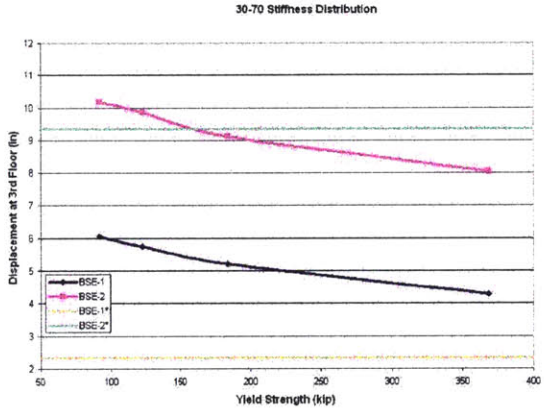

Figure 5-4: Maximum displacement observed on third floor vs. yield strength of dampers for 30-70 stiffness distribution scheme.

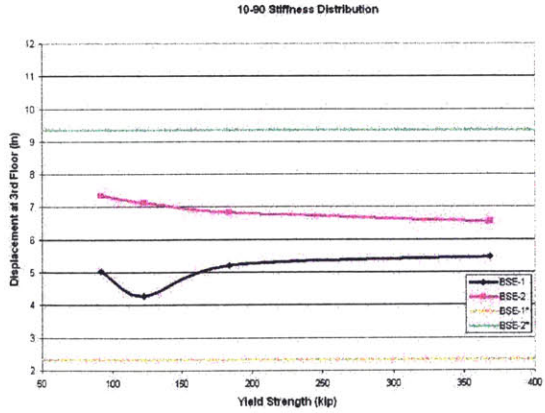

Figure 5-5: Maximum displacement observed on third floor vs. yield strength of dampers for 10-90 stiffness distribution scheme.

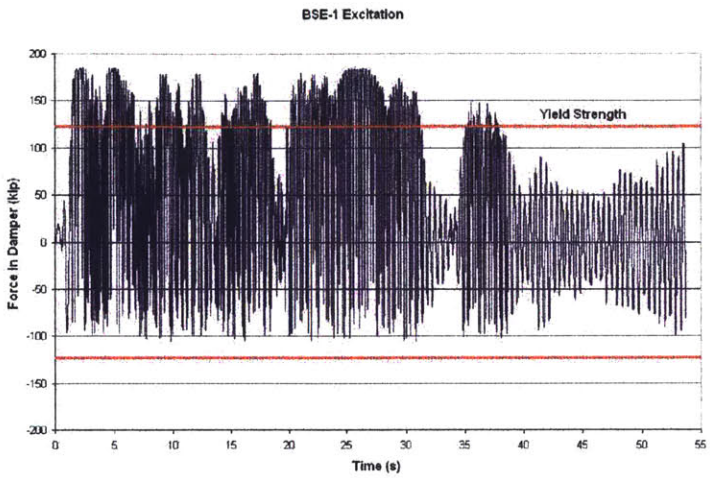

Figure 5-6: Time history of the force the hysteretic dampers (F_{d_y} = 122.8 kips) in the first story experience under BSE-1 excitation.

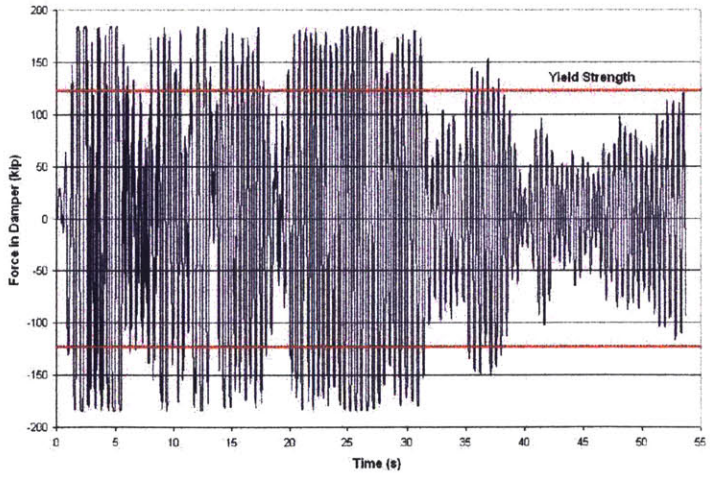

Figure 5-7: Time history of the force the hysteretic dampers (F_{d_y} = 122.8 kips) in the first story experience under BSE-2 excitation.

Chapter 6

Cost Study

An important consideration in every engineering solution is the cost associated with it. As mentioned earlier, the optimal solution to a civil engineering problem is one that provides satisfactory results within the cost limits determined prior to the project. Since this thesis proposes several concepts and methodologies one could follow to attain the desired performance, it is fitting to discuss the cost associated with each of the solutions.

Due to the limited amount information available on costs associated with the design, manufacturing and installation of hysteretic dampers, a very detailed cost analysis will not be presented here. What is of greater interest is the factors affecting the cost of the whole project and their relative importance in the overall cost calculations. In that respect only the costs associated with the hysteretic dampers and the primary lateral support system will be of interest. In addition, no such costs as construction costs will be considered, but rather the material costs will be investigated.

6.1 Cost of the Primary Lateral Support System

The primary lateral support system in this retrofit example consists of pairs of chevron braces, made out of steel. In the construction industry, for ordinary steel, the pricing is done on a per weight units. Hence, determining the weight of the steel used should

be adequate for understanding how the cost varies with stiffness. The process to find the relationship between the stiffness and the cost of the material is presented below:

$C = pW$	p: Price of steel per weight
	C: Cost
	W: Weight of Steel used
$W = \gamma \sum AL$	γ: Weight density of steel
	A: Cross-sectional area
	L: Length of steel
$A = k\frac{L}{2Ecos^2\theta}$	k: Stiffness of each element
	E: Modulus of elasticity for steel
$C = p\gamma \sum \frac{L^2}{2Ecos^2\theta}k$	
$\therefore C = f \sum k$	f: A factor

The final line states that the cost of steel is directly proportional to the sum of the stiffness values provided by these steel members throughout the structure.

6.2 Cost of the Hysteretic Dampers

Establishing a relationship between the cost of hysteretic dampers and the effective damping due to those dampers is more involved than it is for stiffness members. Assuming that Equation 5.4 holds, one can rewrite it as:

$$c_{av} = F_y \frac{4}{\pi \Omega \bar{u}} \left(\frac{\mu - 1}{\mu} \right) \tag{6.1}$$

Assuming the length of the damper is fixed, the amount of damping achieved is a function of the yield strength, which can be correlated to the required area through the yield stress, a material specific parameter. Therefore it can be concluded that damping and cross-sectional area of the hysteretic damper are inversely proportional:

$$c_{av} = g\frac{1}{A}$$

where g is a factor. Assuming the cost is related only to the volume of the yielding material used and the total length of hysteretic dampers is fixed, the cost is inversely proportional to the damping desired on each floor. In other words, the owner would pay less to achieve more damping.

$$Cost = h\frac{1}{c_{av}}$$

In reality however this conclusion will not hold, simply because the cost is not determined only by the amount of material to be used. There are many other factors that need to be incorporated into the cost analysis, such as:

1. Costs associated with using proprietary material.

2. Initial costs incurred in producing and marketing the material.

3. Economies of scale that may prevail if large production facilities exist.

4. The competitiveness in the market for energy dissipation devices.

As hysteretic dampers and energy dissipation devices in general, are relatively new concepts, there are many ambiguities associated with their costs. Enough time needs to pass for hysteretic dampers to become more of a commodity, rather than a proprietary idea, for cost calculations to be as simple and direct as those for steel members.

6.3 Cost of the Retrofit

The different design methodologies presented in Chapter 4 resulted in different combinations of damping and stiffness values that produce an acceptable design. In fact, number of possible stiffness-damping combinations could be increased even further by performing more numerical simulations. Therefore there is no single number for the cost of a retrofit project. To obtain the optimal stiffness-damping combination in terms of cost, one would generate a number of more stiffness-damping combinations that work and then evaluate the cost of each one to determine the lowest cost one.

An additional complexity in the cost calculations exists due to the fact that the hysteretic dampers need to generate stiffness as well as damping for the damping mechanism to function effectively. Since the stiffness provided by the damper is related to its geometric properties such as area and length, there exist many possible designs even for one stiffness-damping combination.

Chapter 7

Conclusion

Studies show that the traditional Strength Based Design methodology is becoming inadequate in responding to the changes in the construction industry, such as the increase in costs of repairs and insurance. As owners become more aware of this fact and attain a better understanding of structural performance levels, there will be a trend towards the use of Damage-Controlled Structures. These structures involve the use of energy dissipation devices to restrict the deformation and therefore the damage of the structure.

The Motion Based Design Approach is recommended here for establishing the stiffness and damping combinations required for the structure's response to be within the design limits. Then cost analysis should be performed to identify the optimal stiffness and damping combination.

The use of hysteretic dampers in Damage-Controlled Structures is common in Japan and is expected to increase in the United States. These devices can be used to attain the optimal stiffness and damping combination that are determined in earlier steps of the design process. However, simulations show that it is difficult to achieve the desired effective damping by using hysteretic dampers due to the assumptions made when expressing hysteretic damping as equivalent viscous damping; a necessary step for the design. In specific, inaccuracies arise due to the fact that the earthquake loads are not periodic functions with constant frequencies.

The effective damping generated by hysteretic dampers is represented by the area

bounded by the Force-displacement curve for the member. Therefore increasing the yield strength of the damper should lead to an increase in the energy dissipation. However, there is a limit to how high the yield strength should be because the hysteretic damper should yield considerably earlier than the primary structure. Finding the optimal yield strength for the hysteretic damper is the main challenge in design process.

The simulations show that the desired response of the three-story structure analyzed in this thesis cannot be achieved by using hysteretic dampers. However, one of the reasons is the impulsive characteristics of the representative earthquake used in the analyses. A wide range of earthquakes should be incorporated into the analysis in order to obtain more reliable conclusions.

Appendix A

Los Angeles Ground Motion Records

Table A.1: 50/50 Set of Records (72 years Return Period). Taken from [3]

Designation	Record Info	Duration (sec)	Magnitude (Mw)	R (km)	Scale	PGA (in/sec^2)
LA41	Coyote Lake, 1979	39.38	5.7	8.8	2.28	227.7
LA42	Coyote Lake, 1979	39.38	5.7	8.8	2.28	128.7
LA43	Imperial Valley, 1979	39.08	6.5	1.2	0.40	55.4
LA44	Imperial Valley, 1979	39.08	6.5	1.2	0.40	43.1
LA45	Kern, 1952	78.60	7.7	107.0	2.92	55.7
LA46	Kern, 1952	78.60	7.7	107.0	2.92	61.4
LA47	Landers, 1992	79.98	7.3	64.0	2.63	130.4
LA48	Landers, 1992	79.98	7.3	64.0	2.63	118.8
LA49	Morgan Hill, 1984	59.98	6.2	15.0	2.35	123.0
LA50	Morgan Hill, 1984	59.98	6.2	15.0	2.35	211.0
LA51	Parkfield, 1966, Cholame 5W	43.92	6.1	3.7	1.81	301.4
LA52	Parkfield, 1966, Cholame 5W	43.92	6.1	3.7	1.81	243.8
LA53	Parkfield, 1966, Cholame 8W	26.14	6.1	8.0	2.92	267.7
LA54	Parkfield, 1966, Cholame 8W	26.14	6.1	8.0	2.92	305.1
LA55	North Palm Springs, 1986	59.98	6.0	9.6	2.75	199.8
LA56	North Palm Springs, 1986	59.98	6.0	9.6	2.75	146.3
LA57	San Fernando, 1971	79.46	6.5	1.0	1.30	97.7
LA58	San Fernando, 1971	79.46	6.5	1.0	1.30	89.2
LA59	Whittier, 1987	39.98	6.0	17.0	3.62	296.7
LA60	Whittier, 1987	39.98	6.0	17.0	3.62	184.7

Table A.2: 10/50 Set of Records (475 years Return Period). Taken from [3]

Designation	Record Info	Duration (sec)	Magnitude (Mw)	R (km)	Scale	PGA (in/sec^2)
LA01	Imperial Valley, 1940	39.38	6.9	10.0	2.01	178.0
LA02	Imperial Valley, 1940	39.38	6.9	10.0	2.01	261.0
LA03	Imperial Valley, 1979	39.38	6.5	4.1	1.01	152.0
LA04	Imperial Valley, 1979	39.38	6.5	4.1	1.01	188.4
LA05	Imperial Valley, 1979	39.08	6.5	1.2	0.84	116.4
LA06	Imperial Valley, 1979	39.08	6.5	1.2	0.84	90.6
LA07	Landers, 1992	79.98	7.3	36.0	3.20	162.6
LA08	Landers, 1992	79.98	7.3	36.0	3.20	164.4
LA09	Landers, 1992	79.98	7.3	25.0	2.17	200.7
LA10	Landers, 1992	79.98	7.3	25.0	2.17	139.1
LA11	Loma Prieta, 1989	39.98	7.0	12.4	1.79	256.9
LA12	Loma Prieta, 1989	39.98	7.0	12.4	1.79	374.4
LA13	Northridge, 1994, Newhall	59.98	6.7	6.7	1.03	261.8
LA14	Northridge, 1994, Newhall	59.98	6.7	6.7	1.03	253.7
LA15	Northridge, 1994, Rinaldi	14.95	6.7	7.5	0.79	206.0
LA16	Northridge, 1994, Rinaldi	14.95	6.7	7.5	0.79	223.9
LA17	Northridge, 1994, Sylmar	59.98	6.7	6.4	0.99	219.9
LA18	Northridge, 1994, Sylmar	59.98	6.7	6.4	0.99	315.5
LA19	North Palm Springs, 1986	59.98	6.0	6.7	2.97	393.5
LA20	North Palm Springs, 1986	59.98	6.0	6.7	2.97	380.9

Table A.3: 2/50 Set of Records (2475 years Return Period). Taken from [3]

Designation	Record Info	Duration (sec)	Magnitude (Mw)	R (km)	Scale	PGA (in/sec^2)
LA21	1995 Kobe	59.98	6.9	3.4	1.15	495.3
LA22	1995 Kobe	59.98	6.9	3.4	1.15	355.4
LA23	1989 Loma Prieta	24.99	7.0	3.5	0.82	161.4
LA24	1989 Loma Prieta	24.99	7.0	3.5	0.82	182.6
LA25	1994 Northridge	14.95	6.7	7.5	1.29	335.3
LA26	1994 Northridge	14.95	6.7	7.5	1.29	364.3
LA27	1994 Northridge	59.98	6.7	6.4	1.61	357.8
LA28	1994 Northridge	59.98	6.7	6.4	1.61	513.4
LA29	1974 Tabas	49.98	7.4	1.2	1.08	312.4
LA30	1974 Tabas	49.98	7.4	1.2	1.08	382.9
LA31	Elysian Park (simulated)	29.99	7.1	17.5	1.43	500.5
LA32	Elysian Park (simulated)	29.99	7.1	17.5	1.43	458.1
LA33	Elysian Park (simulated)	29.99	7.1	10.7	0.97	302.1
LA34	Elysian Park (simulated)	29.99	7.1	10.7	0.97	262.8
LA35	Elysian Park (simulated)	29.99	7.1	11.2	1.10	383.1
LA36	Elysian Park (simulated)	29.99	7.1	11.2	1.10	424.9
LA37	Palos Verdes (simulated)	59.98	7.1	1.5	0.90	274.7
LA38	Palos Verdes (simulated)	59.98	7.1	1.5	0.90	299.7
LA39	Palos Verdes (simulated)	59.98	7.1	1.5	0.88	193.1
LA40	Palos Verdes (simulated)	59.98	7.1	1.5	0.88	241.4

Appendix B

Stiffness Calculations for the Original Structure

Stiffness Calculations for the example building given in FEMA 355C. LA version.

$Ic_A := 3400in^4$ $Ib_1 := 5900in^4$

$Ic_B := 4330in^4$ $Ib_2 := 4930in^4$

$Ic_C := 4330in^4$ $Ib_3 := 1830in^4$

$Ic_D := 3400in^4$ $L_b := 360in$ $E := 29000000psi$

$Ic_E := 723in^4$ $h := 156in$

$$r_{1A} := \frac{Ic_A}{h}\cdot\frac{L_b}{Ib_1} \quad r_{1B} := \frac{Ic_B}{h}\cdot\frac{L_b}{Ib_1} \quad r_{1C} := \frac{Ic_C}{h}\cdot\frac{L_b}{Ib_1} \quad r_{1D} := \frac{Ic_D}{h}\cdot\frac{L_b}{Ib_1}$$

$$r_{2A} := \frac{Ic_A}{h}\cdot\frac{L_b}{Ib_2} \quad r_{2B} := \frac{Ic_B}{h}\cdot\frac{L_b}{Ib_2} \quad r_{2C} := \frac{Ic_C}{h}\cdot\frac{L_b}{Ib_2} \quad r_{2D} := \frac{Ic_D}{h}\cdot\frac{L_b}{Ib_2}$$

$$r_{3A} := \frac{Ic_A}{h}\cdot\frac{L_b}{Ib_3} \quad r_{3B} := \frac{Ic_B}{h}\cdot\frac{L_b}{Ib_3} \quad r_{3C} := \frac{Ic_C}{h}\cdot\frac{L_b}{Ib_3} \quad r_{3D} := \frac{Ic_D}{h}\cdot\frac{L_b}{Ib_3}$$

$$k_{1A} := \frac{12\cdot E\cdot Ic_A}{h^3\left(1+2\cdot r_{1A}\right)} \quad k_{1B} := \frac{12\cdot E\cdot Ic_B}{h^3\left(1+r_{1B}\right)} \quad k_{1C} := \frac{12\cdot E\cdot Ic_C}{h^3\left(1+r_{1C}\right)} \quad k_{1D} := \frac{12\cdot E\cdot Ic_D}{h^3\left(1+2\cdot r_{1D}\right)}$$

$$k_{2A} := \frac{12\cdot E\cdot Ic_A}{h^3\left(1+2\cdot r_{2A}\right)} \quad k_{2B} := \frac{12\cdot E\cdot Ic_B}{h^3\left(1+r_{2B}\right)} \quad k_{2C} := \frac{12\cdot E\cdot Ic_C}{h^3\left(1+r_{2C}\right)} \quad k_{2D} := \frac{12\cdot E\cdot Ic_D}{h^3\left(1+2\cdot r_{2D}\right)}$$

$$k_{3A} := \frac{12\cdot E\cdot Ic_A}{h^3\left(1+2\cdot r_{3A}\right)} \quad k_{3B} := \frac{12\cdot E\cdot Ic_B}{h^3\left(1+r_{3B}\right)} \quad k_{3C} := \frac{12\cdot E\cdot Ic_C}{h^3\left(1+r_{3C}\right)} \quad k_{3D} := \frac{12\cdot E\cdot Ic_D}{h^3\left(1+2\cdot r_{3D}\right)}$$

$k_1 := k_{1A} + k_{1B} + k_{1C} + k_{1D}$ $k_1 = 8.144\times 10^7 \frac{N}{m}$ $k_1 = 4.65\times 10^5 \frac{lbf}{in}$

$k_2 := k_{2A} + k_{2B} + k_{2C} + k_{2D}$ $k_2 = 7.203\times 10^7 \frac{N}{m}$ $k_2 = 4.113\times 10^5 \frac{lbf}{in}$

$k_3 := k_{3A} + k_{3B} + k_{3C} + k_{3D}$ $k_3 = 3.292\times 10^7 \frac{N}{m}$ $k_3 = 1.88\times 10^5 \frac{lbf}{in}$

Bibliography

[1] FEMA–273: NEHRP Guidelines for the Seismic Rehabilitation of Buildings. Technical report, Federal Emergency Management Agency, 1997.

[2] Automated Production of Low Cost Pultruded Composite Bracing for Seismic Energy Dissipation Structures: Phase I Final Technical Report. Technical report, Kazak Composites Incorporated, 2000.

[3] FEMA–355C: Systems Performance of Steel Moment Frames Subject to Earthquake Ground Shaking. Technical report, Federal Emergency Management Agency, 2001.

[4] Parry Brown, Ian D. Aiken, and F. Jeff Jafarzadeh. Seismic retrofit of the Wallace F. Bennett Federal Building. *Modern Steel Construction*, August 2001.

[5] Peter Clark, Ian Aiken, Eric Ko, Kazuhiko Kasai, and Isao Kimura. Design procedures for buildings incorporating hysteretic damping devices.

[6] J. J. Connor. Introduction to Structural Motion Control in progress.

[7] J. J. Connor and A. Wada. Performance based design methodology for structures. In *Proc., Int. Workshop on Recent Developments in Base-Isolation Techniques for Buildings*, Tokyo, Japan, 1992. Arch. Institute of Japan.

[8] J. J. Connor, A. Wada, M. Iwata, and Y.H. Huang. Damage-Controlled Structures. I: Preliminary design methodology for seismically active regions. *Journal of Structural Engineering*, 123(4):423–431, 1997.

[9] A. Wada, J. J. Connor, H. Kawai, M. Iwata, and A. Watanabe. Performance based design methodology for structures. In *Proc., 5th U.S.-Japan Workshop on the Improvment of Build. Struct. Des. and Constr. Practices.* Appl. Technol. Council, 1992.

[10] Akira Wada, Yi-Hua Huang, and Mamoru Iwata. Passive damping technology for buildings in Japan. *Prog. Struct. Engng. Mater.*, (2):335–350, 2000.